Available online at www.sciencedirect.com

ScienceDirect

Mendeleev Commun., 2022, **32**, 645–648

Mendeleev Communications

Tracking nitrogen-to-nickel ratio and prevalent paramagnetic species in synthetic diamonds by electron spin resonance at 90 K

Vladimir Yu. Osipov,*[a] Fedor M. Shakhov,[a] Nikolai M. Romanov[b,c] and Kazuyuki Takai[d]

[a] *Ioffe Institute, 194021 St. Petersburg, Russian Federation. Fax: +7 812 297 1017; e-mail: osipov@mail.ioffe.ru*
[b] *St. Petersburg State Institute of Technology (Technical University), 190013 St. Petersburg, Russian Federation*
[c] *Joint-Stock Company 'Svetlana-Semiconductors', 194156 St. Petersburg, Russian Federation*
[d] *Department of Chemical Science and Technology, Hosei University, Koganei, 184-8584 Tokyo, Japan*

DOI: 10.1016/j.mencom.2022.09.026

Nitrogen and nickel are the main impurities in the type Ib synthetic diamonds obtained under high pressure and high temperature conditions using nickel-containing catalysts. Nitrogen enters the synthesized diamond from the air. The nickel/nitrogen ratio for the two types of diamonds, obtained with and without an aluminum getter that prevents the diamond crystal lattice from nitrogen penetration, was studied by electron spin resonance at 90 K.

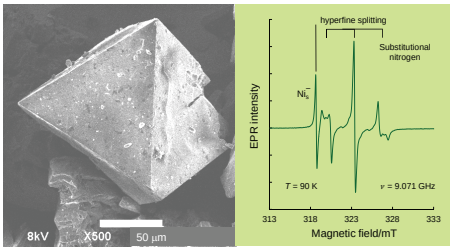

Keywords: synthetic diamond, impurities, high pressure and high temperature, electron spin resonance, solid state chemistry, analytical chemistry.

The synthesis of diamonds from graphite and graphite-like materials in high-pressure apparatuses was discovered in the mid-1950s and is still a developing industrial technology that uses the latest achievements in this field situated at the intersection of physics and solid-state chemistry.[1,2] A huge number of studies are devoted to the problem of impurities (and related centers) in synthetic diamonds and the purity of crystals. In addition, some centers act as color ones, giving intense luminescence in the green and red spectral regions.[3] This issue is also the subject of analytical chemistry.

Synthetic diamonds are usually grown from carbon raw materials in high-pressure chambers with the addition of an iron–manganese or an iron–nickel catalyst to the batch.[4] The selection of these metals is based on the fact that carbon dissolves well in them at temperatures above 1300 °C. In practice, when crystals are grown using an iron–nickel catalyst, they contain nickel (in a concentration of up to 20 ppm), along with iron. Nitrogen penetrates the growing crystal from atmospheric air located in the high-pressure cell itself and adsorbed on particles of a carbon material mixed with a catalyst. Its concentration can vary from 100 to 700 ppm. To control the technological process, it is extremely important to monitor the content of nitrogen, nickel and other transition metals in the grown diamond crystals. The growth of diamonds using a nickel-only catalyst melt is also possible and has been well studied.[5,6] As for two-component catalysts, the dissolution of carbon in a nickel catalyst melt is important. The growth of diamonds using a pure nickel catalyst was mainly applied to obtain diamonds containing Ni-based or polyatomic nitrogen–nickel impurity complexes appeared immediately after synthesis or during subsequent annealing above 1600 °C.[6–8] Some of them have outstanding luminescent properties. In this case, the adjustment of the nitrogen content in the crystals was achieved by introducing a certain amount (~ 2%) of a nitrogen getter (for example, titanium or zirconium) into a melt metal catalyst. It takes place because the getter binds to nitrogen and keeps it in the solution, therefore, it enters the growing diamond lattice in a smaller amount.[9]

There are many different methods for studying the elemental composition of samples. Some of them, for example, inductively coupled plasma mass spectroscopy, are very sensitive to the impurity composition and accurate (at the level of ppm), while the other, like SEM–EDS (scanning electron microscopy with energy dispersive X-ray spectroscopy), are very insensitive to transition metals and rough (an accuracy of 0.5%). It is often required to have one inexpensive method for estimation of impurity components concentration in diamond. Electron paramagnetic resonance (EPR) appears to be such a method with respect to nitrogen and nickel impurities. EPR signals from nitrogen and nickel in synthetic and/or natural diamonds were first detected and identified by Smith *et al.*[10] in 1961 and Isoya *et al.*[9,11] in 1990, respectively. The signal from paramagnetic nitrogen is readily observed at room temperature and has a triplet structure associated with the magnetic moment of ^{14}N (I = 1), the splitting between the satellites is about 70 Gauss. The spin state of nitrogen in the neutral state is S = 1/2. The signal from substitutional nickel impurity in the −1 charge state appears only at temperatures below 120 K. The corresponding Lorentzian-shaped EPR signal with a g-factor of 2.0319 is labelled W8.[12] The spin state of this complex is S = 3/2. Nickel is an acceptor impurity in diamond. In the neutral substitutional state (N_s^0), its spin equals two, and when an electron is captured (Ni_s^-), it becomes 3/2 with electronic configuration $3d^7$.[9,11] Here we do not consider the case of nickel atoms in the interstices of diamond lattice, which have electronic spins S = 0 ($3d^{10}$ configuration) and S = 1/2 ($3d^9$ configuration) in the neutral or charged +1 states.[8] The latter is usually less than 6% of the total number of

nickel impurities, especially in the case of a significant amount of nitrogen impurities (more than 100–120 ppm) in the system.

In this work, we analyzed the EPR spectra of the two samples synthesized at the Ioffe Institute using a high-pressure chamber[13] at high temperature. In one case, only graphite and nickel as a catalyst were loaded into the high-pressure chamber, and in the other case, aluminum was added as a getter of atomic nitrogen.† For more details, see Online Supplementary Materials and ref. 14. Aluminum readily binds to nitrogen during the synthesis and thereby reduces the content of nitrogen impurity in the substitutional state in the obtained diamond crystals. The almost optimal percentages of the used powder mixtures were chosen for syntheses and the possible deviations of the mixture compositions are not so important for the subsequent analysis of the impurities in the grown diamond crystals being 40–160 μm in size. For this reason, we do not examine the effect of the composition of Ni–C and Al–Ni–C mixtures on the content of the main impurities and quality of the crystals formed. It should only be noted that after the completion of the syntheses, the crystals were extracted from the batch by etching off the metal phase in hot acids with subsequent washing with boiling water. Microcrystalline powders synthesized without and with aluminum are denoted below as MD1 and MD2, respectively.

SEM images of the synthesized diamonds are shown in Figure S1 (see Online Supplementary Materials). The grown microcrystals have an arbitrary shape for the both samples, far from regular faceting, although a small amount of almost ideal crystals of octahedral and other shapes could be found. These microcrystals with good octahedral faceting and (111) faces also show small surface macro-defects in the form of terraces and voids. Overall, the type MD2 microcrystals are more perfect due to a less defective internal structure.

Figure 1 shows the EPR spectra‡ of samples MD1 and MD2 recorded at 90 K. The both spectra clearly show the triplet signals from paramagnetic nitrogen (P1 centers) together with the isolated Lorentzian-shaped signals from a nickel defect Ni_s^- in the −1 charge state in the low-field spectral region. The spectrum of the MD2 sample consists of narrow lines, while the broad ones are observed in the spectrum of the MD1 sample. The latter is due to the broadening of the EPR lines of all paramagnetic agents due to the presence of a broadening paramagnetic agent in the system. In this case, the broadening agent is paramagnetic nitrogen. Therefore, the EPR spectrum of the sample obtained without an aluminum getter that binds nitrogen atoms is a superposition of equally broadened lines with linewidth up to 2.2 mT. Here we mean the full width at half maximum (FWHM) $\Delta H_{1/2}$ for each component of the true EPR spectrum, although

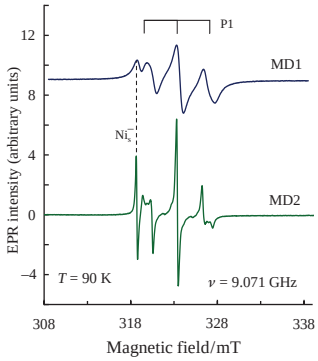

Figure 1 EPR spectra of samples MD1 (grown without aluminum) and MD2 (grown with aluminum) recorded at 90 K.

for spectra of the first derivative of microwave absorption, the linewidth is usually represented by the peak-to-peak distance ΔH_{pp}, which in the case of Lorentzian-shaped lines is related to $\Delta H_{1/2}$ by the formula: $\Delta H_{pp} = \Delta H_{1/2}/1.7321$. Actually, the EPR spectrum of the MD2 sample consists of a set of narrow lines: a triplet from nitrogen and a Lorentzian-shaped line from Ni_s^-. For the correct deconvolution of the EPR spectra of each sample into separate components, each spectrum was integrated [Figures 2(*a*) and 3] and the integral spectra were deconvoluted into separate plots.

Figure 2(*b*) shows the deconvolution of the spectrum of the MD1 sample into the components arising from nitrogen, nickel Ni_s^- and one more defect. Here, the spectrum consists of five components with Lorentzian line shapes and the fitting was made by selecting 15 variable parameters, of which the widths and amplitudes of individual components are fundamental, and the positions of the components are determined elementarily. Due to the large self-broadening of the lines because of a high concentration of paramagnetic impurities (mainly nitrogen), the signal from nitrogen consists of three equally spaced Lorentzian-shaped lines with an approximate intensities ratio of 1:1:1 [blue line in Figure 2(*b*)]. In this case, there is also an intensive signal from the third paramagnetic agent [orange plot in Figure 2(*b*)] in the vicinity of the central line (g = 2.0024). Its linewidth (ΔH_{pp})

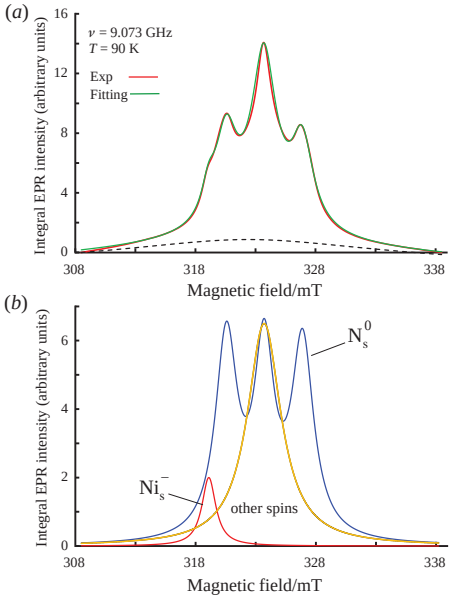

Figure 2 (*a*) Integral EPR spectrum of sample MD1 and (*b*) its deconvolution into components to determine the ratio of the concentrations of substitutional nickel and nitrogen impurities. The dashed line in panel (*a*) is the background drawn to better fit the integral EPR spectrum with the corresponding two Lorentzian-shaped singlets (red and orange plots) and a triplet of the overlapping almost identical Lorentzian-shaped lines (blue).

† The mixtures of graphite (50 wt%) and nickel (50 wt%) powders or graphite (45.5 wt%), nickel (45.5 wt%) and aluminum (9 wt%) powders (with particle sizes ~350 μm, < 70 μm and <140 μm, respectively) were loaded into the inner space of a toroidal high-pressure chamber. The synthesis was performed under pressure of 5–5.5 GPa at 1650 °C for 90 s. The obtained crystals were below 130 μm in size.

‡ EPR spectra were recorded at room temperature and at 90 K at microwave frequency of ~9.5 GHz using X-band EPR spectrometer JEOL JES-FA 300 (Japan). Diamond powder in an amount of ~ 10–12 mg was introduced into a quartz capillary with an outer diameter of 2.1 mm sealed at the lower end, and the sample was placed in a standard quartz EPR tube with an outer diameter of 5 mm. The upper end of the capillary was also isolated from the external atmosphere. The spectra (absorption first derivative) of the samples were recorded at a microwave power of 3 μW in a mode very far from the saturation of the EPR signal. The recording range was from 300 to 350 mT on the magnetic field scale. For quantitative estimation of the paramagnetic centers' concentration, the spectra were integrated with the subsequent estimation of the areas under the corresponding plots (in particular, those having Lorentzian line shapes) of the integrated spectrum.

is 1.96 mT. The latter can be associated with centers of non-nitrogen origin, for example, negatively charged vacancies, and with compact paramagnetic clusters based on several nitrogen atoms. Similar signals with g = 2.0024–2.0027 arising from the deconvolution of EPR signals from P1 centers into their components were also observed earlier for other specially fabricated diamond systems.[15,16] Their precise assignment is difficult because of many alternatives. However, elucidation of the nature of this paramagnetic agent [orange plot in Figure 2(*b*)] is beyond the scope of this article. The signal from nickel is well recognized in Figure 2(*b*) as the small adjacent Lorentzian-shaped curve (centered at 319.1 mT) overlapping with the low-field satellite of the triplet signal from nitrogen (P1). The ratio of the integrated signal intensities for nickel and nitrogen is about 0.077. In this case, the intensity of the integral signal for nitrogen is determined by the all three equally broadened components centered at ~320.56, ~323.7 and ~326.9 mT.

The spectrum of sample MD2 after integration is shown in Figure 3. The central line of the signal from nitrogen and the line from the nickel defect have Lorentzian shapes. But the lines of the nitrogen signal satellites have a peculiar shape due to the random distribution of the crystal axes of the microcrystals in the powder relative to the direction of the magnetic field. However, this does not affect the ability to integrate the signal from nitrogen (P1). The ratio of the integral intensities of the components of the P1 triplet is about 1:1:1 (Figure 3). This allows us to estimate the total integral intensity of the signal from nitrogen using only the integral intensity of one high-field component (from 325.3 to 329 mT) taken with a factor of 3. A similar estimate can be made using the integral intensity of both satellite components from the nitrogen triplet signal and a conversion factor of 1.5. The Lorentzian-shaped signal (g = 2.0319) from Ni_s^- (highlighted in green) is perfectly integrated, and it stands apart in Figure 3. The ratio of the integrated signal intensities for Ni_s^- and nitrogen for sample MD2 is 0.081, approximately as that for sample MD1. The estimated nitrogen concentration in sample MD2 is ~133 ppm according to the van Wyk approach proposed for synthetic diamonds doped with nitrogen.[17,§] This estimate is based on an analysis of the linewidth ΔH_{pp} ~ 0.146 mT for the central line with g = 2.0024 (at T = 293 K) and on the assumption that the prevailing part (>70%) of paramagnetic centers in the MD2 diamond is due to the substitutional nitrogen. The procedure is carried out by plugging the experimentally found EPR linewidth

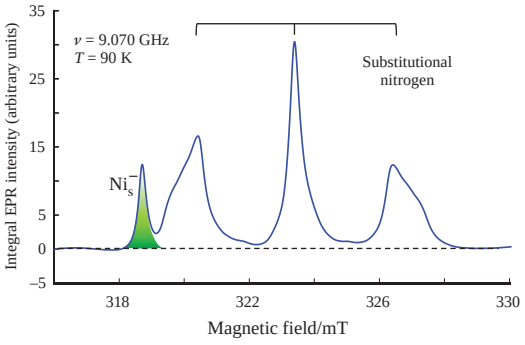

Figure 3 EPR spectrum of sample MD2 at 90 K after integration. The Lorentzian plot due to the signal from nickel is highlighted in green. The nitrogen concentration was determined from the area below the both satellites of the triplet taken with the appropriate conversion factor. A small background passing under all the signals was specially subtracted to achieve approximately equal integral intensities (1:1:1) of the triplet components.

§ The empirical formula of van Wyk was proposed to describe the triplet EPR spectra (linewidths of nitrogen-doped diamond) recorded at room temperature. In the approximation of a weak temperature dependence of the linewidths, this formula is also valid for the range of 90–300 K.

into the equation from the work of van Wyk *et al*. and determining the desired concentration of centers. The empirical formula used is quite simple:

$$\Delta H_{pp}[\mathrm{G}] = (1.2 \times 10^{-4} N_s^2 + 0.014)^{1/2}, \quad (1)$$

where ΔH_{pp} is the linewidth (peak-to-peak distance) expressed in Gauss units and N_s is the paramagnetic center concentration in ppm.[17]

The estimate for the MD1 sample based on ΔH_{pp} ~ 0.77 mT (measured at 293 K) gives ~700 ppm for all paramagnetic species with S = 1/2 and S = 3/2 together. For this estimate, we used EPR data obtained at room temperature rather than those obtained at low temperature, namely ΔH_{pp} ~ 0.813 mT (measured at 90 K). Thus, an increase in the concentration of all paramagnetic species by a factor of ~5 results in a broadening of the central component of the triplet near g ~ 2.0024 by the same factor, approximately the same as for the signal of nickel centers, where its ΔH_{pp} increased from 0.15 mT to 0.81 mT. But not all spins from this estimate (~700 ppm) belong to isolated nitrogen centers. Some of them belong to defects of an extraneous type, possibly with a spin of 1/2. This is clearly seen from the central part of the integrated EPR spectrum of the MD1 sample [Figure 2(*a*)] and the result of the deconvolution of this spectrum into components [Figure 2(*b*)]. After subtracting the integral contribution from the components (orange and red singlets) not associated with the substitutional nitrogen (~ 40%) to the EPR spectrum, it has ~ 420 ppm of the estimated substitutional nitrogen.

Let us examine the situation with the integrated intensity of the EPR line from Ni_s^- in more detail. Ni_s^- has a spin S_1 of 3/2. Therefore, there are three possible transitions with Δm_s = 1 with coincided resonance frequencies (here Δm_s is a change in the magnetic quantum number m_s) upon absorption of a quantum of the microwave radiation. These transitions are as follows: $-1/2 \rightarrow +1/2$, $-3/2 \rightarrow -1/2$, and $+1/2 \rightarrow +3/2$ (Figure S2, top part). The positions of the EPR lines from the second and third transitions are indistinguishable from that for the line of the main transition $-1/2 \rightarrow +1/2$ on the magnetic field scale, so the one broadened line appears in the spectrum. The integral intensity of this line (A_1) is proportional to the concentration of nickel impurity in the −1 charge state.

For paramagnetic nitrogen having S_2 = 1/2, there is one type of microwave transition with Δm_s = 1, *viz*. $-1/2 \rightarrow +1/2$. Due to the presence of the nitrogen atom with nucleic magnetic moment I = 1 it splits into three microwave transitions between the six corresponding levels while maintaining the nuclear magnetic quantum number m_I = +1; 0 or −1 (Figure S2, bottom part). The integral intensity (A_2) of the EPR signal from the nitrogen centers P1 (together with the side satellites) is determined by three intervals along the magnetic field scale and is proportional to the number of neutral nitrogen (N_s) sites in the system. Here, the subscript 's' denotes the substitutional type of the nitrogen impurity (or P1 center) in the lattice.

Thus, the integral intensities of the EPR lines for the P1 and Ni_s^- centers are determined by the shapes of the corresponding lines (bands). At the same time, the nitrogen center with spin S_2 = 1/2 and the nickel center with spin S_1 = 3/2 give microwave absorption differing by several times. Useful ideas for comparing microwave absorption from spins of different magnitudes, which form simple or complex centers depending on the environment, were proposed earlier.[18–21] The coefficient taking into account this difference was calculated to be $S_1(S_1+1)/[S_2(S_2+1)] = 5$.[20,21] That is, the ratio of the integral intensities (A_1/A_2) of the EPR signals for spins of both types (S_1 = 3/2 and S_2 = 1/2) is related to the ratio of the concentrations (N_1/N_2) of these spins in the material as follows:¶

$$\frac{A_1}{A_2} = \frac{N_1}{N_2}\frac{S_1(S_1+1)}{S_2(S_2+1)}\frac{g_1^2}{g_2^2} = 5\frac{N_1}{N_2}\frac{g_1^2}{g_2^2}. \quad (2)$$

Here $g_{1,2}$ are the Lande-factors of the EPR signals from substitutional nickel and nitrogen, and we can assume that the ratio g_1^2/g_2^2 is ~ 1.

Therefore, the use of factor 5 to recalculate the ratio of the concentrations of the 1/2 and 3/2 spins from the ratio of the intensities of their EPR signals gives the concentration of Ni_s^- spins in sample MD2 equal to

$$N_1 = N_2 \frac{A_1}{A_2} \cdot \frac{1}{5} = 133 \text{ ppm} \times 0.081 \times 1/5 \approx 2.2 \text{ ppm}, \quad (3)$$

and for sample MD1:

$$N_1 = 420 \text{ ppm} \times 0.077 \times 1/5 \approx 6.5 \text{ ppm}. \quad (4)$$

The obtained concentrations of the hetero-elements $[N_s] = N_2 = 133$ ppm and $[Ni_s^-] = N_1 = 2.2$ ppm are surprisingly close to the values of 134 ppm and 2 ppm given for the Ib HPHT diamond made according to the standard factory technology using nickel-containing catalyst.[24] However, for a sample with a high nitrogen concentration, obtained without a getter, the content of nickel in the Ni_s^- state has already increased proportionally. This suggests that the presence of an aluminum getter in the catalytic melt during the synthesis decreases not only the nitrogen content, but also the nickel content in the grown crystallites. The probable mechanism of action of aluminum on carbon in the Ni–Al catalytic melt is as follows. Dissolved aluminum covers the emerging diamond nuclei with a thin layer, through which carbon is transferred from the melt to the growing diamond, while nitrogen is not transferred, and partially binds to aluminum in the layer. Thus, we can say that aluminum is not so much a nitrogen getter, but its separator. The aluminum enriched layer may have a similar effect on the transfer of nickel from the melt to the growing diamond nucleus (see Figure S3).

The described method for determining the concentration of nickel in diamond (in the range up to 20 ppm) can be used in production, when assessing the quality of diamond crystals grown with nickel centers as optical centers, and also as a method of analytical chemistry for independent detection of this element in low concentrations. In this regard, microcrystalline diamond powder with nickel at a concentration below 3 ppm can serve as a reference standard for calibrating other elemental analysis methods sensitive to 3d metals.

In addition, the results obtained for the EPR signal of substitutional nickel can also be applied to the analysis of nickel as an internal impurity in the crystal lattice of diamond particles 5–30 nm in size, although small particles attach 3d transition metal cations to their outer shell of oxygen-containing groups to a much greater extent.[25,26] This work also focuses on the protocol for obtaining quantitative data on paramagnetic impurities in diamonds, compared to studies that do not use this aspect in the analysis of EPR spectra.[27]

In this work, EPR signals from nitrogen and nickel, which occupy substitutional positions in the diamond lattice, were observed together at temperatures below 100 K. Signals from these centers are similarly broadened depending on the concentration of paramagnetic centers prevailing in the system. Such broadening agents for the Ib HPHT diamonds are isolated centers of paramagnetic nitrogen, which are present in the studied samples at concentrations of 420 ppm and ~130 ppm. The lower $[N_s]$ value is achieved by introducing ~10 wt% aluminum into a graphite–nickel mixture held at high temperature and high pressure. The concentration of paramagnetic nickel in the Ni_s^- state turns out to be ~60 times less than the concentration of nitrogen for the both samples.

V.O. and F.S. thank the Ioffe Institute for support (project 0040-2014-0013). K.T. acknowledges the support of JSPS KAKENHI (grant nos. 16K05758, 19K05410 and 26107532). The authors are grateful to Mr. F.M. Kochetkov for his help in preparing the samples. The diamond samples were synthesized as part of a research cooperation between the Disco Corporation (Tokyo, Japan) and the Ioffe Institute. EPR measurements at low temperatures were carried out with the support of the Hosei University (Japan).

Online Supplementary Materials

Supplementary data associated with this paper can be found in the online version at doi: 10.1016/j.mencom.2022.09.026.

References

1 A. A. Giardini and J. E. Tydings, *Am. Mineral.*, 1962, **47**, 1393.
2 S. M. Stishov, *Phys.-Usp.*, 2019, **62**, 704 (*Usp. Fiz. Nauk*, 2019, **189**, 752).
3 A. M. Zaitsev, *Optical Properties of Diamond. A Data Handbook*, Springer-Verlag, Berlin, Heidelberg, 2001.
4 I. A. Dobrinets, V. G. Vins and A. M. Zaitsev, *HPHT-Treated Diamonds*. *Diamonds Forever* (*Springer Series in Materials Science*, vol. 181), Springer-Verlag, Berlin, Heidelberg, 2013.
5 S. Yamaoka, H. Komatsu, E. Iizuka, O. Fukunaga and N. Setaka, *J. Ceram. Assoc. Jpn.*, 1977, **85**, 73 (*Yogyo Kyokai-shi*, 1977, **85**, 73).
6 R. N. Pereira, A. J. Neves, W. Gehlhoff, N. A. Sobolev, L. Rino and H. Kanda, *Diamond Relat. Mater.*, 2002, **11**, 623.
7 H. Kanda and K. Watanabe, *Diamond Relat. Mater.*, 1999, **8**, 1463.
8 R. N. Pereira, W. Gehlhoff, A. J. Neves and N. A. Sobolev, *J. Phys.: Condens. Matter*, 2003, **15**, 2493.
9 J. Isoya, H. Kanda and Y. Uchida, *Phys. Rev. B: Condens. Matter Mater. Phys.*, 1990, **42**, 9843.
10 W. V. Smith, P. P. Sorokin, I. L. Gelles and G. J. Lasher, *Phys. Rev.*, 1959, **115**, 1546.
11 J. Isoya, H. Kanda, J. R. Norris, J. Tang and M. K. Bowman, *Phys. Rev. B: Condens. Matter Mater. Phys.*, 1990, **41**, 3905.
12 A. T. Collins, H. Kanda, J. Isoya, C. A. J. Ammerlaan and J. A. van Wyk, *Diamond Relat. Mater.*, 1998, **7**, 333.
13 F. M. Shakhov, A. M. Abyzov, S. V. Kidalov, A. A. Krasilin, E. Lähderanta, V. T. Lebedev, D. V. Shamshur and K. Takai, *J. Phys. Chem. Solids*, 2017, **103**, 224.
14 F. M. Shakhov, V. Yu. Osipov, A. A. Krasilin, K. Iizuka and R. Oshima, *J. Solid State Chem.*, 2022, **307**, 122804.
15 V. Yu. Osipov, F. M. Shakhov, K. V. Bogdanov, K. Takai, T. Hayashi, F. Treussart, A. Baldycheva, B. T. Hogan and C. Jentgens, *Nanoscale Res. Lett.*, 2020, **15**, 209.
16 V. Yu. Osipov, F. M. Shakhov, N. N. Efimov, V. V. Minin, S. V. Kidalov and A. Ya. Vul', *Phys. Solid State*, 2017, **59**, 1146 (*Fiz. Tverd. Tela*, 2017, **59**, 1125).
17 J. A. van Wyk, E. C. Reynhardt, G. L. High and I. Kiflawi, *J. Phys. D: Appl. Phys.*, 1997, **30**, 1790.
18 V. Yu. Nagy, *Anal. Chim. Acta*, 1997, **339**, 1.
19 V. Yu. Nagy, P. N. Komozin and M. F. Desrosiers, *Anal. Chim. Acta*, 1997, **339**, 31.
20 N. D. Yordanov, *Appl. Magn. Reson.*, 1994, **6**, 241.
21 D. Siebert, J. Dahlem and V. Nagy, *Anal. Chem.*, 1994, **66**, 2640.
22 G. E. Pake and T. L. Estle, *The Physical Principles of Electron Paramagnetic Resonance*, 2nd edn., W. A. Benjamin, Reading, MA, 1973, p. 152.
23 C. P. Poole, Jr., *Electron Spin Resonance: A Comprehensive Treatise on Experimental Techniques*, 2nd edn., Wiley, New York, 1983, p. 409.
24 O. A. Shenderova, A. I. Shames, N. A. Nunn, M. D. Torelli, I. Vlasov and A. Zaitsev, *J. Vac. Sci. Technol., B: Nanotechnol. Microelectron.: Mater., Process., Meas., Phenom.*, 2019, **37**, 030802.
25 V. Yu. Osipov, N. M. Romanov, I. E. Suvorkova, E. V. Osipova, T. Tsuji, Y. Ishiguro and K. Takai, *Mendeleev Commun.*, 2022, **32**, 132.
26 I. D. Gridnev and V. Yu. Osipov, *Mendeleev Commun.*, 2022, **32**, 143.
27 V. Yu. Dolmatov, A. N. Ozerin, I. I. Kulakova, O. O. Bochechka, N. M. Lapchuk, V. Myllymäki and A. Vehanen, *Russ. Chem. Rev.*, 2020, **89**, 1428.

Received: 21st March 2022; Com. 22/6832

¶ See, for example, equation (12)[21], where S_1 and S_2 should be substituted. The methodological explanations given there[21] in the process of deriving this formula are very valuable. The fundamentals and intermediate equations for deriving this simple relation had been given.[22,23]